Infrared, Raman and high-frequency dielectric spectroscopy and the phase transitions in $Na_{1/2}Bi_{1/2}TiO_3$

2004 J. Phys.: Condens. Matter 16 2719

(http://iopscience.iop.org/0953-8984/16/15/022)

INSTITUTE OF PHYSICS PUBLISHING JOURNAL OF PHYSICS: CONDENSED MATTER

J. Phys.: Condens. Matter **16** (2004) 2719–2731 PII: S0953-8984(04)75065-1

Infrared, Raman and high-frequency dielectric spectroscopy and the phase transitions in $Na_{1/2}Bi_{1/2}TiO_3$

J Petzelt[1], S Kamba[1], J Fábry[1], D Noujni[1], V Porokhonskyy[1], A Pashkin[1], I Franke[2], K Roleder[2], J Suchanicz[3], R Klein[4] and G E Kugel[4]

[1] Institute of Physics, Academy of Sciences of the Czech Republic, Na Slovance 2, 182 21 Praha 8, Czech Republic
[2] Institute of Physics, University of Silesia, Ulica Uniwersytecka 4, 40-007 Katowice, Poland
[3] Institute of Physics, Pedagogical University, Ulica Podchorazych 2, 30-084 Krakow, Poland
[4] MOPS Laboratory, FRE CNRS 2304, University of Metz and Supelec, 2 rue Edouard Belin, 57-078 Metz, France

Received 16 January 2004
Published 2 April 2004
Online at stacks.iop.org/JPhysCM/16/2719
DOI: 10.1088/0953-8984/16/15/022

Abstract

Infrared reflectivity, time-domain terahertz transmission, high-frequency dielectric measurements and Raman spectroscopy of $Na_{0.5}Bi_{0.5}TiO_3$ complex ferroelectric perovskite were performed in a broad temperature range. The results were analysed considering the macroscopic symmetry as well as symmetry resulting from local Na–Bi ordering in all three known phases. An overdamped infrared soft mode was revealed in the THz range which, together with central-mode type dispersion in the GHz range, contribute to the strong and broad dielectric permittivity maximum around 600 K. Anharmonic Bi and/or Na vibrations and local hopping, respectively, are suggested to be the main origins of these excitations. The broad phonon spectra and the frequency independent dielectric losses at low temperatures are compatible with the existence of nanoscopic polar regions and disorder to liquid He temperatures similar to relaxor ferroelectrics.

1. Introduction

Sodium bismuth titanate $Na_{0.5}Bi_{0.5}TiO_3$ (NBT) belongs to one of a few ferroelectric complex perovskite-type compounds with two different ions at the A site of the ABO_3 structure. Although it has been known for quite a long time [1], it has recently attracted attention as an environmentally friendly lead-free compound which exhibits attractive piezoelectric properties [2, 3]. Moreover, it undergoes a very peculiar sequence of phase transitions (PTs) [4], and shows unusual dielectric [3–9] and ferroelectric [2, 4, 6] properties. The temperature

dependent dielectric response in pure NBT shows a broad anomaly with a somewhat smeared maximum of the low-frequency relative permittivity near 593 K reaching values of about 3000 [3, 4, 6], with the low temperature (at 5 K) value of ∼125 (in ceramics [10]) or almost 200 (in crystals [11]). Dielectric relaxations below the MHz range were observed at higher temperatures [5, 8], but were shown to be due to finite conductivity effects [7, 9]. No dielectric studies above 1 MHz are known to the authors. Similarly, except for an early mid-infrared (IR) study on powdered samples [12], to the authors' knowledge no other IR data have been published. On the other hand, several Raman studies have been published, both on single crystals [13–18] as well as ceramics [19, 20]. Very important data for understanding the two known high-temperature phase transitions and their dynamics (see below) has been obtained by inelastic neutron scattering [4, 21].

2. Experiment

NBT ceramics were prepared via the conventional mixed oxide route, starting from high-quality Na_2CO_3, Bi_3O_2 and TiO_2 powders [8].

IR reflectivity spectra from a polished BNT ceramic pellet were obtained using a Fourier transform spectrometer Bruker IFS 113v, in the frequency range of 30–3000 cm^{-1} (0.9–90 THz) at room temperature, and only up to 650 cm^{-1} at low temperature (down to 10 K) limited by the transparency region of the polyethylene windows used in the Optistat CF cryostat (Oxford Instruments). High-temperature spectra up to 430 K were obtained using a custom-made furnace. Pyroelectric deuterated triglycine sulfate detectors were used for the room- and high-temperature measurements, while a sensitive cooled (1.5 K) Si bolometer was used for the low-temperature experiment.

THz transmission measurements were performed using a femtosecond amplified laser system with two [110] ZnTe plates used to generate (by non-linear optic rectification) and detect (by electro-optic sampling) the THz pulses [22]. Our THz technique allows us to determine the complex dielectric response $\varepsilon^*(\omega)$ in the range of 3–80 cm^{-1}, the actual spectral range depending on the transparency of the investigated sample. The ceramic platelet used in this study was 100 μm thick which allowed us to determine the low-temperature spectra in the 3–30 cm^{-1} range.

IR reflectivity spectra were fitted, together with the $\varepsilon^*(\omega)$ THz spectra, using a generalized-oscillator model with the factorized form of the complex dielectric function

$$\varepsilon^*(\omega) = \varepsilon'(\omega) - \mathrm{i}\varepsilon''(\omega) = \varepsilon_\infty \prod_{j=1}^{n} \frac{\omega_{\mathrm{LO}j}^2 - \omega^2 + \mathrm{i}\omega\gamma_{\mathrm{LO}j}}{\omega_{\mathrm{TO}j}^2 - \omega^2 + \mathrm{i}\omega\gamma_{\mathrm{TO}j}}, \tag{1}$$

where $\varepsilon^*(\omega)$ is related to reflectivity $R(\omega)$ by

$$R(\omega) = \left| \frac{\sqrt{\varepsilon^*(\omega)} - 1}{\sqrt{\varepsilon^*(\omega)} + 1} \right|^2. \tag{2}$$

$\omega_{\mathrm{TO}j}$ and $\omega_{\mathrm{LO}j}$ are the transverse and longitudinal frequencies of the jth mode, respectively, and $\gamma_{\mathrm{TO}j}$ and $\gamma_{\mathrm{LO}j}$ are the respective damping constants. The high-frequency permittivity ε_∞ results from electronic absorption processes much above phonon frequencies (in the UV–vis range).

High-frequency dielectric measurements in the frequency range of 1 MHz–1.8 GHz and temperature range 100–570 K were performed with a HP 4291B impedance analyser and Novocontrol BDS 2100 coaxial sample cell with a small cylindrical sample (∼5 mm long and 0.5 mm in diameter) at the end of the shortened coaxial line. The complex dielectric function was calculated taking into account the electromagnetic field distribution in the sample [23].

Raman spectroscopy was carried out on two multi-domain crystal samples in the temperature range 10–820 K using a Spex-double monochromator model 1401. The unpolarized spectra were fitted by a sum of the classical oscillator spectral function to determine the parameters of the phonon modes.

3. Structure, phase transitions and symmetry considerations

NBT undergoes (at least) two structural PTs on cooling from the prototypic high-temperature cubic phase. The most recent powder neutron diffraction data [24] do not show considerable A-site ion ordering so that the distribution of Na and Bi ions can be taken to be random and the averaged (macroscopic) symmetry is that of the simple cubic perovskite, $Pm\bar{3}m$ (O_h^1) with one formula unit per unit cell ($Z = 1$). On cooling from high temperatures, around $T_1 \cong 820$ K, a first-order antiferrodistortive PT to the tetragonal polar phase $P4bm$ (C_{4v}^2), $Z = 2$, occurs [25]. Both phases coexist in some temperature interval (783–813 K). From the viewpoint of Landau theory, such a PT can be realized by a combination of two three-component order parameters [4, 21] transforming according to the M_3^+ irreducible representation at the Brillouin zone point $\boldsymbol{k} = (1/2, 1/2, 0)\boldsymbol{a}^*$ (and other two equivalent points under the constraint that only one component—namely at that single $\boldsymbol{k}$-point—is non-zero) [26–28] and according to the polar F_{1u} irreducible representation at the Brillouin-zone centre Γ-point (under the constraint that only the c component is non-zero, permitting the P_c direction of the spontaneous polarization). Freezing of the former parameter leads to $a^0a^0c^+$ TiO_6-octahedra tilting (corresponding to Glazer's notation [29] with in-phase tilt of all octahedra about the c axis), freezing of the latter one to $\boldsymbol{k} = 0$ c-direction shifts of all atoms. Unlike in the usual tetragonal ferroelectric perovskites, these shifts show a prevailing antiferroelectric pattern in Bi/Na and Ti cations with a weak polar (ferrielectric) component [24]. Comparing the structure at 673 K with the cubic one, the c displacements of Bi/Na with respect to Ti are 0.18 Å and with respect to O atoms 0.12–0.14 Å, whereas the a and b displacements of the corresponding O atoms describing the octahedral tilts are ∼0.12 Å. Since the critical neutron scattering in the cubic phase was observed mainly at the M point, and at lower temperatures at the R point (connected with the second PT), the F_{1u}-symmetry order parameter seems to be the secondary one triggered by the condensation of the primary M_3^+ parameter. The PT can therefore be classified as triggered ferroelectric and improper ferroelastic [30, 31], but it can be also called ferrielectric. This explains why no appreciable dielectric anomaly is observed near T_1 and no first-order IR (nor Raman) active soft mode could be expected in the cubic phase.

The second PT occurs around $T_2 \approx 593$ K. It is also of first order but diffuse and connected with a broad coexistence of both phases (∼530–690 K [32, 24]). The low-temperature phase is rhombohedral (space group $R3c$ (C_{3v}^6), $Z_{prim} = 2$), which is not a subgroup of the tetragonal phase, but it can be related to the cubic phase as its subgroup. Again, two order parameters are needed to describe the distortion from the cubic phase. One is at the R point of the Brillouin zone ($\boldsymbol{k} = (1/2, 1/2, 1/2)\boldsymbol{a}^*$, irreducible representation R_4^+ with all three frozen components equal). Freezing of this parameter describes equal anti-phase tilting of neighbouring octahedra about all crystallographic axes $a^-a^-a^-$. The second order parameter has again F_{1u} symmetry at the Γ point like the polarization, but all frozen components are non-zero and equal to each other, which give rise to spontaneous polarization along the cube body diagonal ($P_a = P_b = P_c$). The PT with respect to the cubic phase is again triggered ferroelectric and improper ferroelastic, but P_s is much higher than in the tetragonal phase [2]. This is comparable to proper ferroelectrics, because (unlike the tetragonal phase) all cations undergo in-phase polar shifts [24]. This implies a strong coupling (from the symmetry only bi-quadratic [21] in the Landau-type thermodynamic potential for the cubic phase) between the R_4^+ and F_{1u} order parameters

and probably also strong (also bi-quadratic) coupling between the M_3^+ and R_4^+ and M_3^+ and F_{1u} parameters. This is supported by neutron-scattering results [21] in which the critical (unresolved) quasielastic scattering appeared near both the R and Γ points in the tetragonal phase only, with extrapolated critical temperatures of ∼610 and ∼490 K, respectively. This could be due to the freezing of the M_3^+ order parameter which (through the coupling) triggers the R- and Γ-point instability. The Γ-point instability is also revealed by the increase of the permittivity down to ∼600 K with an extrapolated Curie–Weiss temperature of ∼490 K, which agrees with the neutron data. Nevertheless, the correlation length of ferroelectric fluctuations remains finite even below the permittivity maximum (∼7 nm) and only slightly increases (up to ∼11 nm) on cooling down to room temperature [4]. This indicates that no proper long-range ferroelectric order is reached. Additional neutron scattering studies [33] revealed an incommensurate modulation along the tetragonal *c* axis which appears near 600 K and survives down to low temperatures (at least 100 K). The modulation period is temperature independent with the mean period of ∼5 nm in the purely rhombohedral phase below ∼400 K. It was assigned to quasi-periodic anti-phase nanodomains. In addition to the A-site disorder, due to the modulation the rhombohedral phase in NBT remains disordered down to low temperatures.

The factor-group analysis (see table 1) for the cubic $Pm\bar{3}m$ phase predicts $3F_{1u}$ polar (IR active, but Raman inactive) modes and $1F_{2u}$ silent (IR and Raman inactive) modes, all triply degenerate. In the tetragonal phase $P4bm$ (disordered Na, Bi in Wyckoff position 2b, Ti and OI in 2a, OII in 4c) the factor-group analysis yields $4A_1(\mathrm{IR, R}) + 3A_2(-) + 1B_1(\mathrm{R}) + 3B_2(\mathrm{R}) + 8\mathrm{E(IR, R)}$ optic modes (IR and R mean activity in IR and Raman spectra, respectively). Hence, 12 modes are simultaneously active in IR and Raman spectra and four are only Raman active modes. We note that this result differs from the factor-group analysis published in [20]. The triply degenerate F_{1u} and F_{2u} modes from the cubic phase should split into $A_1 + E$ and $B_1 + E$ doublets, respectively. This represents three strong IR and simultaneously weak Raman doublets generated from the F_{1u} modes and one weak Raman doublet and one weak IR mode generated from the silent F_{2u} mode. The remaining $1A_1 + 3B_2 + 4E$ modes generated from the M point should give rise to additional weak Raman modes, out of which the A_1 and E modes should be also weakly IR active.

In the rhombohedral phase $R3c$ (disordered Na, Bi in Wyckoff position 2a, Ti in 2a and O in 6b) the factor-group analysis yields $4A_1(\mathrm{IR, R}) + 5A_2(-) + 9\mathrm{E(IR, R)}$ optic modes, which represents in total 13 simultaneously IR and Raman active modes. Again, this result is at variance with that in [20]. The three strong cubic IR modes should again split into three strong IR and simultaneously weak Raman doublets (generally with frequencies differing from those in the tetragonal phase) and the silent mode will generate only a weak IR and Raman singlet. The remaining $1A_1 + 6E$ modes originated from the R point should give rise to additional IR and simultaneously Raman weakly active modes (again generally differing from the modes of the tetragonal phase).

In the case of the disordered cubic phase $Pm\bar{3}m$, no first-order Raman spectrum is expected. However, the high-temperature single-crystal Raman spectra [14, 15] show a low-frequency (20–30 cm^{-1}) first-order Raman line of F_{2g} symmetry surviving on heating up to ∼1000 K. Therefore Siny *et al* [14, 15] suggested that some local A-site ordering is present in the NBT crystal, at least below this temperature. This was also assumed by Park *et al* [34] on the basis of x-ray studies, even though no direct measurements in the cubic phase were presented in their paper. In the case of ordered regular alteration of Na and Bi ions, they suggest the local symmetry with space group $Fm\bar{3}m$ ($Z = 8$, $Z_{\mathrm{prim}} = 2$). The factor group analysis then yields the following optic modes: $A_{2u}(-) + E_u(-) + 5F_{1u}(\mathrm{IR}) + F_{2g}(\mathrm{R}) + 2F_{2u}(-)$. So, one F_{2g} triply degenerate Raman mode is expected in the spectra, in agreement with the above experiment. The factor group analysis shows that its eigenvector corresponds only to

Table 1. Factor-group analysis of the lattice vibrations in the three phases of NBT assuming A-site disorder as well as regular Na–Bi ordering.

$Na_{1/2}Bi_{1/2}TiO_3$				
(a) A-site disorder				
	T_2 (K)		T_1 (K)	
$R3c$ (C_{3v}^6)	530	$P4bm$ (C_{4v}^2)	773	$Pm\bar{3}m$ (O_h^1)
$Z_{prim} = 2$		$Z = 2$	−813	$Z = 1$
$a^-a^-a^-$		$a^0a^0c^+$		
Triggered		Triggered		
Ferroelectric		Ferroelectric		Parent
Improper		Improper		(prototype)
Ferroelastic		Ferroelastic		
2(Na, Bi) 2Ti } —2 · 2a		2(Na, Bi)—2b		Na, Bi—1b F_{1u}
		2Ti 2OI } —2 · 2a		Ti—1a F_{1u}
6O—6b		4OII—4c		O—3d $2F_{1u} + F_{2u}$
$4A_1$(IR + R)		$4A_1$(IR + R)		$3F_{1u}$ (IR)
$5A_2(-)$		$3A_2(-)$		$1F_{2u}(-)$
9E(IR+R)		$1B_1$(R)		
		$3B_2$(R)		Soft phonon mode
		8E(IR+R)		at M-point
13(IR + R)		12(IR + R) + 4(R)		3(IR) + 0(R)
(b) A-site order				
$R3$ (C_3^4)		$P4_2nm$ (C_{4v}^4)		$Fm\bar{3}m$ (O_h^5)
$Z_{prim} = 2$		$Z = 4$		$Z_{prim} = 2$
Proper ferroelectric		Triggered ferroelectric		Parent
Improper ferroelastic		Improper ferroelastic		
Na + Bi—2 · 3a		2Na 2Bi } 2 · 2a		Na—4a F_{1u} Bi—4b F_{1u}
$Ti_1 + Ti_2$—2 · 3a		4Ti + $4O_1$—2 · 4b		2Ti—8c $F_{1u} + F_{2g}$
3(OI + OII)—2 · 9b		$4O_5 + 4O_6$—2 · 4c		6O—24d $A_{2u} + E_u + 3F_{1u} + 2F_{2u}$
9A(IR + R)		$7A_1$(IR + R)		$A_{2u}(-)$
9E(IR + R)		$4A_2(-)$		$E_u(-)$
		$4B_1$(R)		F_{2g}(R)
		$8B_2$(R)		$5F_{1u}$(IR)
		17E(IR + R)		$2F_{2u}(-)$
18(IR + R)		24(IR + R) + 12(R)		5(IR) + 1(R)

Ti displacements along the (111) direction, in opposite directions in adjacent TiO_6 octahedra. This is in accord with its low frequency.

One can ask what would be the structure of both low-temperature phases combining the A-site ordering with the distortions discussed above. Our crystallographic considerations show that for the tetragonal phase the resulting space group is $P4_2nm$ (C_{4v}^4), $Z = 4$ (Na and Bi in 2a sites, Ti and O1 in 4b sites, O5 and O6 in 4c sites). The factor-group analysis of the optic modes then yields: $7A_1(IR, R) + 4A_2(-) + 4B_1(R) + 8B_2(R) + 17E(IR, R)$. Because the doubling of the primitive unit cell is present as in the disordered case, the transition from the cubic phase is triggered ferroelectric and improper ferroelastic also in the local sense, since similar two order parameters as in the disordered case are needed to describe the symmetry change $Fm\bar{3}m \rightarrow P4_2nm$.

However, in the case of the rhombohedral phase our considerations yield the space group $R3$ (C_3^4), $Z_{\mathrm{prim}} = 2$ (Na, Bi, Ti1, Ti2 in 3a sites, O1 and O2 in 9b sites). The factor-group analysis for optic modes yields 9A(IR, R) + 9E(IR, R) and, unlike in the disordered case, there is no doubling of the primitive unit cell with respect to the ordered cubic phase. Looking for the order parameter for the (now equitranslational) $Fm\bar{3}m \rightarrow R3$ transition, it turns out that one needs two parameters, namely one of F_{1u} symmetry (with the constraint that all its three components condense in the same way) and another one of A_{2u} symmetry. The one-dimensional A_{2u} parameter originates from the R_4^+ parameter of the half-sized Brillouin zone corresponding to the disordered $Pm3m$ phase, whereas the frozen F_{1u} parameter has the same meaning in the ordered as well as disordered structure—it merely describes the shift of all atoms in the (111) direction. Comparing the room temperature structure with the cubic-phase structure one obtains shifts along P_S for Bi/Na ions about 0.17 Å and for Ti ions 0.09 Å (in the same direction) with respect to the O_6–octahedra framework. Perpendicular to P_S, displacements (mainly in the x-axis direction of the hexagonal coordinate system) concern only O atoms and amount to ∼0.23 Å. This means that freezing of both the order parameters is comparable and it is difficult to decide merely from the structure at room temperature which of the parameters is the primary one from the point of view of the Landau theory (see the discussion about the order-parameter coupling above). Nevertheless, from the viewpoint of local symmetry, the rhombohedral phase represents a proper ferroelectric phase with respect to the cubic one, which allows us to understand better the pronounced dielectric anomaly (Curie–Weiss law) and high P_S.

Recently, from Raman studies [20] and diffuse x-ray scattering [35], it was suggested that other possible nanoclusters could form, e.g. with $NaTiO_3$ and $BiTiO_3$ segregation. We do not see convincing Raman arguments [20] for the appearance of such clusters, moreover they are incompatible with the local requirements for electro-neutrality and therefore are not likely. Still another possible nano-ordering was recently suggested in [35]. It concerns the displacement of Bi ions (in our view Na ions as well) off the [111] axis in the (001) directions, which would decrease the local symmetry to the monoclinic space group Cm. Similar displacements were observed also in Pb-ion relaxors [36]. However, this symmetry breaking should be not only local, but also temporal because, like in the case of Pb relaxors, the Bi(Na) ions are assumed to perform fast hopping among these displaced sites, preserving the time averaged rhombohedral structure. Nevertheless, in principle it may also influence the x-ray diffuse scattering and Raman and IR selection rules, in addition to the possible appearance of a relaxational central mode in the Raman and IR spectra due to strong anharmonic Bi(Na) vibrations (hopping). It seems to be difficult to distinguish between the two types of local ordering (static Na–Bi or Na–Na, Bi–Bi clusters from correlated dynamic Bi(Na) hopping), but Kreisel *et al* [35] claim that the possible Na–Bi ordering is de-correlated from the observed nanopolar zones in NBT. This is probably true also in classical relaxors (PMN, PLZT) since the local compositional (chemical) order is frozen at common temperatures (below ∼1000 K), whereas polar clusters develop only below the Burns temperature (typically ∼600 K) and grow on cooling [37]. In the case of NBT we shall assume that the polar regions are actually basically due to the large anharmonic Bi(Na) vibrations and are revealed in our dielectric spectra (see below).

4. Results and discussion

In figure 1 we present our IR reflectivity spectra at selected temperatures together with their fit, performed simultaneously with the time domain THz data. The complex dielectric function calculated from the fit parameters, together with the selected THz data, is shown in figure 2. It is clearly seen that the most pronounced temperature changes appear in the low-frequency range

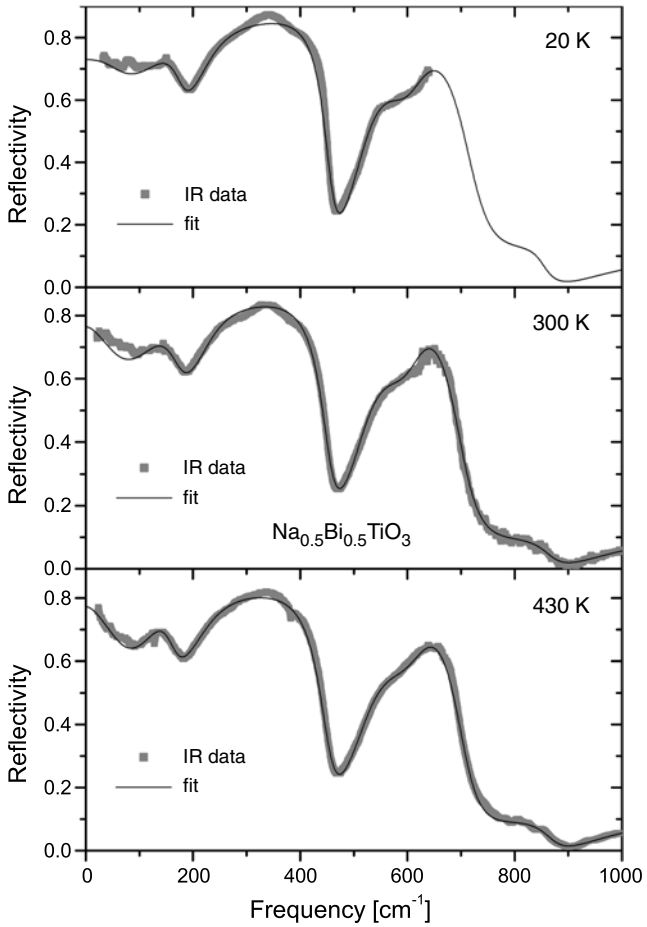

Figure 1. IR reflectivity spectra of NBT ceramics at selected temperatures. Solid curves show the fit (see text).

above 100 K and concern the strong soft mode region. The fit shows that the soft mode (probably its lower-frequency E-symmetry component) remains heavily damped or overdamped at all temperatures (on increasing temperature from 10 to 430 K, the eigenfrequency drops from 55 to 45 cm^{-1}, whereas the damping constant increases from 95 to 120 cm^{-1}). In such a case the eigenfrequency ω_{SM} and damping γ_{SM} become strongly correlated and the fit is not fully unambiguous. The most significant experimental quantity in such a case is the frequency of the maximum of loss function $\varepsilon''(\omega)$ which lies approximately at $\omega_R = \omega_{SM}^2/\gamma_{SM}$, which in the limit of very high damping corresponds to the Debye relaxation frequency. The plot of this frequency against temperature shows (within the limit of experimental accuracy) its approximate linear softening with extrapolated softening temperature ~600 K, corresponding to the permittivity maximum. This is a strong indication that our IR soft mode is the origin of the dielectric anomaly and the ferroelectric PT dynamics. A similar mode with a similar extrapolated softening temperature was also observed in single-crystal Raman spectra below room temperature [14, 17].

The three main IR modes (active also in the cubic phase) are presumably near 140, 233 and 520 cm^{-1} (the mode at 140 cm^{-1} overlaps with the A_1 soft mode); the additional two modes

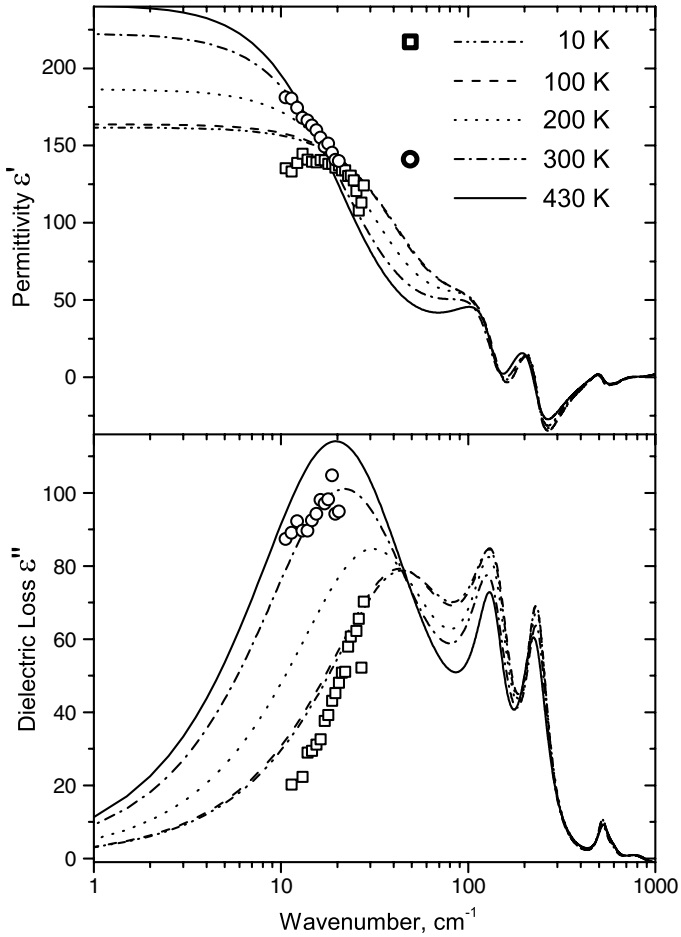

Figure 2. Complex dielectric functions calculated from the fit in figure 1 at selected temperatures together with THz data at extreme measured temperatures.

allowed by the local ordering are the ferroelectric soft mode and the mode at 827 cm^{-1}. Their splitting in the rhombohedral phase is not resolved, apparently due to their high damping.

The results of our HF dielectric measurements are presented in figures 3 and 4 as a function of temperature and frequency, respectively. The permittivity monotonically increases with temperature, but in agreement with low-frequency data [3, 7, 9] no temperature maximum is reached up to 560 K. It is clearly seen that some dispersion sets in at high temperatures, but its characteristic relaxation frequency is above our high-frequency limit. From comparison of figures 2, 4 and the published low-frequency permittivity data [10] it follows that at the lowest (liquid He) temperature the IR soft mode accounts for the whole value of low-frequency permittivity, but on increasing temperature a growing continuous loss background appears in the whole HF range and moreover an additional central-mode type dispersion emerges at the HF end at high temperatures.

The constant loss spectrum below room temperature (so-called $1/f$ noise) and the corresponding weak logarithmic permittivity dispersion, were recently observed and analysed in PLZT [38] and other relaxor ferroelectrics. It is connected with the highly anharmonic dynamics in polar nanocluster boundary regions influenced by strong random fields, enabling

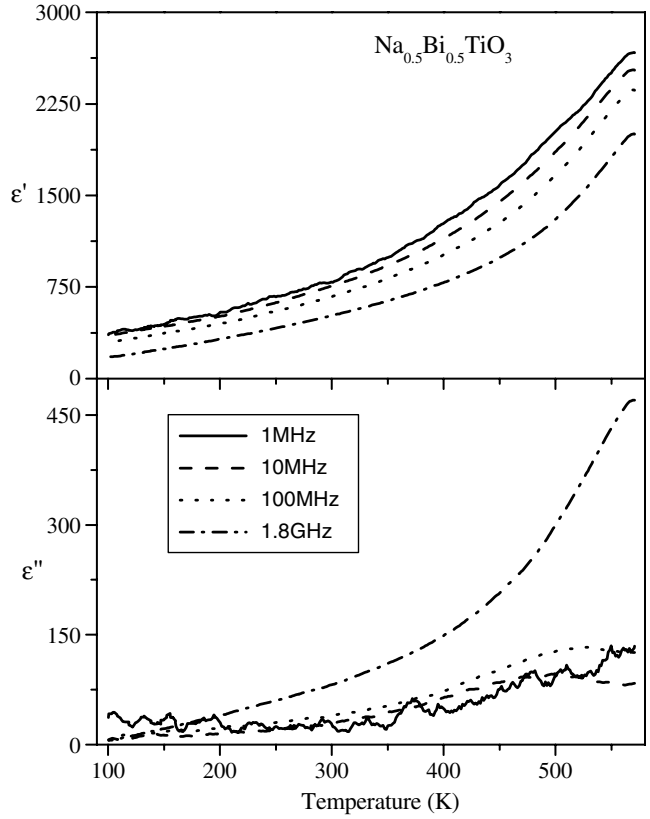

Figure 3. Temperature dependences of the NBT permittivity and losses at different HF frequencies.

their large volume fluctuations (breathing) and it seems to be present in all disordered ferroelectrics. The additional central-mode type microwave dispersion appears above room temperature, unfortunately above our high-frequency limit (1.8 GHz). Assuming a Debye relaxation model for this dispersion, our estimate based on the HF and THz data yields the corresponding relaxation frequency at 430 K in the 5–10 GHz range and its dielectric strength $\Delta\varepsilon_{CM} \cong 500$. At higher temperatures $\Delta\varepsilon_{CM}$ should increase up to 1000–2000 and its frequency should somewhat decrease, still staying above 2 GHz.

Our single crystal Raman spectra at selected temperatures between 10 and 823 K are presented in figure 5. The spectra are in general agreement with other published Raman data [14, 15, 18]. The E-symmetry soft mode is seen in our as well as other Raman spectra [14, 17], together with its split-off A_1 (A) component (at $\sim$150 cm^{-1}) [13]. As required by symmetry, both these modes disappear in the cubic phase from both IR and Raman spectra. Let us pay particular attention to the low-frequency part of the spectra at low temperatures where a slightly resolved doublet is seen. We assign it to the E-symmetry soft mode coupled with the F_{2g} mode from the cubic phase. The F_{2g} mode (consisting of anti-polar Ti vibrations), which is activated in Raman spectra due to the local ordering, is seen at $\sim$25 cm^{-1} in the cubic phase (up to 1000 K according to [15]) and on cooling it hardens to $\sim$44 cm^{-1} at 10 K. At low temperatures it clearly couples with the soft mode (both have the same E symmetry) and anti-crosses it in the 20–60 K range, as evidenced by the intensity transfer between the modes. However, detailed behaviour of both the modes in a broader temperature range cannot

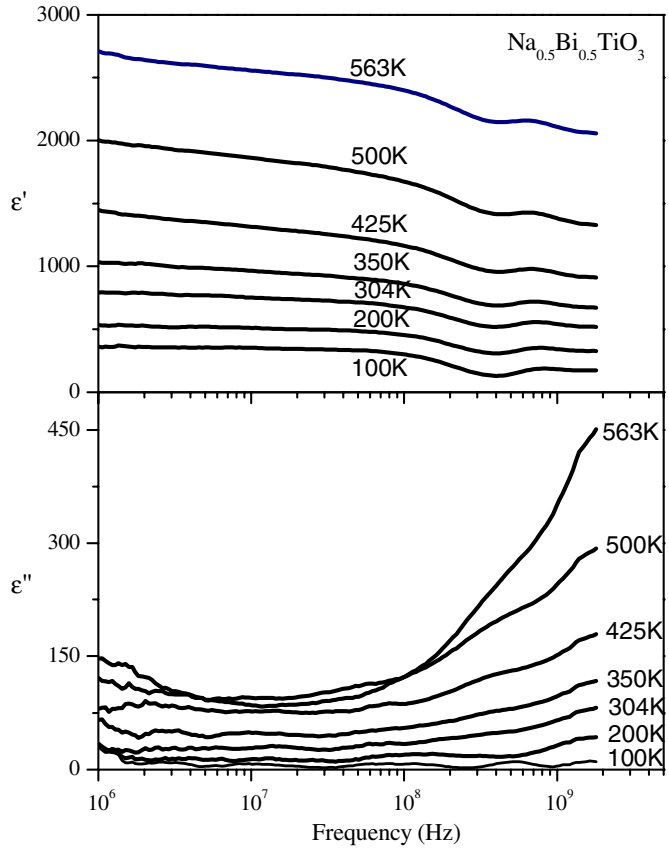

Figure 4. Frequency dependences of the complex HF dielectric response at different temperatures. (This figure is in colour only in the electronic version)

be unambiguously deduced from our data. We only see that the behaviour agrees with that from IR spectra within the accuracy limit except for somewhat higher damping in the IR case. This could be due to the polycrystallinity of our sample for IR measurements. The Raman modes near 140 and 530 cm^{-1} are probably the main IR modes activated due to the breaking of the inversion. Also the broad Raman feature near 800 cm^{-1} corresponds probably to the weak IR mode.

In the Raman spectra the central mode also appears and dominates at high temperatures peaking up near ∼650 K [18], slightly higher than the dielectric permittivity, or, according to [16] at practically the same temperature. Its roughly estimated frequency lies in the 300 GHz range [18]. The central-peak background was also observed in Brillouin scattering spectra [39], and another much narrower component was suggested [18]. This is probably the analogue of the dielectric central mode in the GHz range, whereas the broader Raman central mode at higher temperatures corresponds to our overdamped IR soft mode.

Concerning the microscopic assignment of the soft and central mode, it is usual to assume that both have the same eigenvector, corresponding in our case predominantly to Bi(Na)-ion vibrations against the TiO_6 octahedra. The soft mode concerns the quasi-harmonic vibrations within a single potential well at each of the six assumed local Bi(Na) sites displaced in the (001)

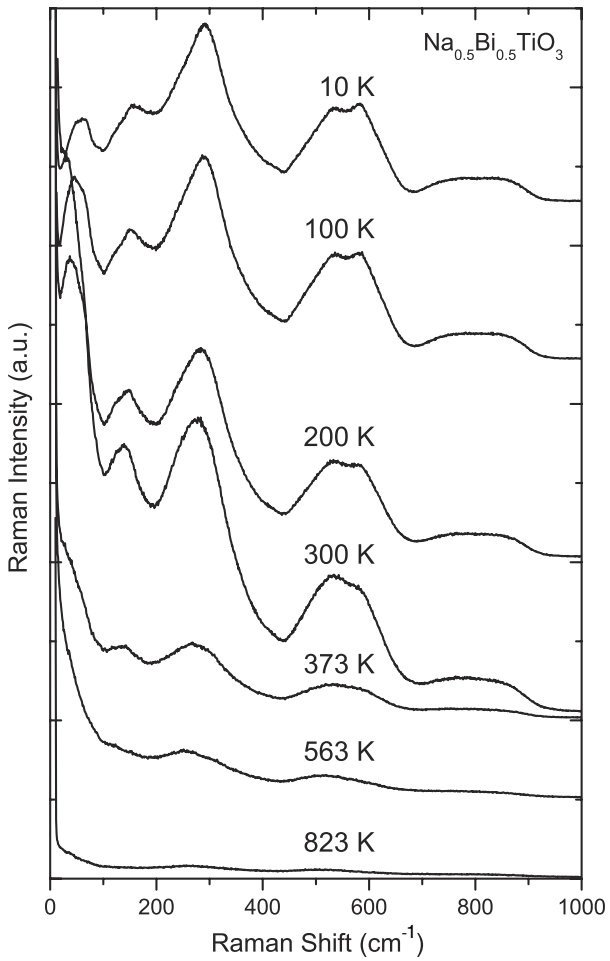

Figure 5. Unpolarized Raman spectra of the NBT crystal at selected temperatures.

directions from the mean rhombohedral site, whereas the central mode corresponds to hopping of Bi(Na) ions among the local sites. Its unusually low frequency might be influenced by the collective character of such a hopping, forming in this way the dynamic polar clusters. The disappearance of the central mode below room temperature can be understood as correlated freezing of the Bi(Na) displacements off the rhombohedral sites in one of the (001) directions. Different polar clusters then correspond to different off-rhombohedral (001) displacements. The estimate based on a model for diffuse x-ray scattering performed in [35] yields flat disc-like clusters of 1 nm $\times$ 20 nm size. The diffuse neutron scattering yields their characteristic size of 11 nm at room temperature and $\sim$7 nm at 550 K [4]. By analogy with PLZT [38] we can then interpret the frequency independent losses at low temperatures to breathing (volume fluctuations) of the frozen polar clusters.

The low-frequency permittivity maximum near 600 K, which corresponds to the region of co-existence of the tetragonal and rhombohedral phases, is obviously connected with the maximal strength of the central mode. To understand its microscopic picture in this temperature range, we have to assume that both phases are intermixed in a nanoscopic way so that the central

mode should correspond to hetero-phase fluctuations, as also suggested by Siny *et al* [18]. Unlike usual relaxors, where in the range of maximum permittivity the dielectric dispersion has already set in at low frequencies providing in this way the characteristic relaxor behaviour, in NBT the main dispersion appears only in the GHz range. Therefore in the standard dielectric measurements up to 1 MHz no typical relaxor behaviour occurs and the relaxor behaviour (shift of the permittivity versus temperature maxima with frequency) can be expected only in the HF and microwave range.

Finally, we have to comment on the expected soft mode behaviour in the range of both PTs and in the cubic phase, where our measurements are missing so far. It appears that, as in relaxor ferroelectrics [40, 41], the soft mode does not account for the main part of the permittivity in the range of the permittivity maximum. The dominant contribution comes from the additional strong microwave dispersion due to the polar cluster re-orientation (at higher temperatures) and breathing (at lower temperatures). A similar situation concerning the small contribution of the soft mode to the dielectric anomaly appears in NBT. The extrapolated soft mode softening near 600 K cannot be expected to occur completely, taking into account the coupling with the central mode which takes over the softening near the permittivity maximum [42]. So its softening should cease in this temperature range, and at sufficiently high temperatures (in the cubic phase) one can expect merging of the central mode into the soft mode response, as happens in the case of usual relaxors above the Burns temperature [41]. One should take into account that the soft mode in the cubic phase is IR active only due to the local symmetry breaking (ordering) so that it should appear anyway as an overdamped and probably not very strong feature. High temperature THz measurements are needed to characterize this behaviour more quantitatively.

5. Conclusions

The phase transition sequence in NBT was analysed and classified according to the macroscopic and local symmetry, assuming local Na–Bi ordering. The corresponding factor-group analysis of all phases was performed. The IR soft mode behaviour in NBT was analysed and the broad dielectric anomaly around 600 K was decomposed into the overdamped soft mode and central mode contribution in the THz and 2–10 GHz range, respectively. The soft mode dominates in the dielectric response at low temperatures up to room temperature, whereas above ∼400 K the central-mode contribution prevails. It was suggested that both the excitations concern mainly the highly anharmonic Bi and/or Na vibrations and hopping among the off rhombohedral sites. The dynamics of the PTs in NBT belongs therefore to the crossover between the displacive and order–disorder behaviour. Unfortunately, direct microwave data in the main GHz relaxation region are still missing. At low temperatures, the nearly frequency independent loss spectrum was observed similarly to relaxor ferroelectrics. The spectroscopic data support the local Na–Bi ordering even in the high-temperature cubic phase, but the broad phonon spectra (together with the frequency-independent losses) speak for a strong lattice disorder down to low temperatures, in agreement with structural studies.

Acknowledgments

The authors thank V Dvorak for a critical reading the manuscript and helpful discussions. The work was supported by the Grant Agency of the Czech Republic (project no 202/04/0993) and Czech Academy of Sciences (projects A1010213, AVOZ1-010-914 and K1010104).

References

[1] Smolensky G A, Isupov V A, Agranovskaya A I and Krainik N N 1960 *Sov. Phys.—Solid State* **11** 2982
[2] Emelianov S M, Rayevsky I P, Smotrakov V G and Savenko F I 1984 *Fiz. Tverd. Tela* **26** 1897 (in Russian)
[3] Roleder K, Franke I, Glazer A M, Thomas P A, Miga S and Suchanicz J 2002 *J. Phys.: Condens. Matter* **14** 5399
[4] Vakhrushev S B, Isupov V A, Kvyatkovsky B E, Okuneva N M, Pronin I P, Smolensky G A and Syrnikov P P 1985 *Ferroelectrics* **63** 153
[5] Tu C-S, Siny I G and Schmidt V H 1994 *Phys. Rev.* B **49** 11550
[6] Park S E, Chung S J and Kim I T 1996 *J. Am. Ceram. Soc.* **79** 1290
[7] East J and Sinclair D C 1997 *J. Mater. Sci. Lett.* **16** 422
[8] Suchanicz J 1998 *Mater. Sci. Eng.* B **55** 114
[9] Saradhi B V B, Srinivas K, Prasad G, Suryanarayana S V and Bhimasankaram T 2003 *Mater. Sci. Eng.* B **98** 10
[10] Suchanicz J, Jezowski A and Poprawski R 1998 *Phys. Status Solidi* a **169** 209
[11] Suchanicz J, Jezowski A, Poprawski R and Dacko S 2000 *Phys. Status Solidi* b **221** 789
[12] Kaleveld E W, Bruntinck D J, Dotman J P and Blasse G 1973 *J. Inorg. Nucl. Chem.* **35** 3928
[13] Zhang M-S and Scott J F 1986 *Ferroelectr. Lett.* **6** 147
[14] Siny I G, Smirnova T A and Kruzina T V 1991 *Ferroelectrics* **124** 207
[15] Siny I G, Smirnova T A and Kruzina T V 1991 *Sov. Phys.—Solid State* **33** 61
[16] Gavshin M G and Pastukhov V I 1998 *Ferroelectrics* **205** 81
[17] Lushnikov S G, Gvasaliya S N, Siny I G, Sashin I L, Schmidt V H and Uesu Y 2000 *Solid State Commun.* **116** 41
[18] Siny I G, Husson E, Beny J M, Lushnikov S G, Rogacheva E A and Syrnikov P P 2001 *Physica* B **293** 382
[19] Kreisel J, Glazer A M, Bouvier P and Lucazeau G 2001 *Phys. Rev.* B **63** 174106
[20] Kreisel J, Glazer A M, Jones G, Thomas P A, Abello L and Lucazeau G 2000 *J. Phys.: Condens. Matter* **12** 3267
[21] Vakhrushev S B, Kviatkovski B E, Malysheva R S, Okuneva N M, Platchenova E L and Syrnikov P P 1989 *Kristallografiya* **34** 154
[22] Kuzel P and Petzelt J 2000 *Ferroelectrics* **239** 949
[23] Grigas J 1996 *Microwave Dielectric Spectroscopy of Ferroelectrics and Related Materials* (Amsterdam: Gordon and Breach)
[24] Jones G O and Thomas P A 2002 *Acta Crystallogr.* B **58** 168
[25] Jones G O and Thomas P A 2000 *Acta Crystallogr.* B **56** 426
[26] Dvorak V 1963 *Phys. Status Solidi* **3** 2235
[27] Aleksandrov K S and Bartolome J 2001 *Phase Transitions* **74** 255
[28] Stokes H T, Kisi E H, Hatch D M and Howard C J 2002 *Acta Crystallogr.* B **58** 934
[29] Glazer A M 1972 *Acta Crystallogr.* B **28** 3384
[30] Dvorak V 1974 *Ferroelectrics* **7** 1
[31] Holakovsky J 1973 *Phys. Status Solidi* b **56** 615
[32] Suchanicz J and Kwapulinski J 1995 *Ferroelectrics* **165** 249
[33] Vakhrushev S B 1997 *Doctor Thesis* St Petersburg
[34] Park S-E, Chung S-J, Kim I-T and Hong K S 1994 *J. Am. Ceram. Soc.* **77** 2641
[35] Kreisel J, Bouvier P, Dkhil B, Thomas P A, Glazer A M, Welberry T R, Chaabane B and Mezouar M 2003 *Phys. Rev.* B **68** 014113
[36] Dkhil B, Kiat J M, Calvarin G, Baldinozzi G, Vakhrushev S B and Suard E 2002 *Phys. Rev.* B **65** 024104
[37] Mihailova B, Bismayer U, Güttler B, Gospodinov M and Konstantinov L 2002 *J. Phys.: Condens. Matter* **14** 1091
[38] Rychetsky I, Kamba S, Porokhonskyy V, Pashkin A, Savinov M, Bovtun V, Petzelt J, Kosec M and Dressel M 2003 *J. Phys.: Condens. Matter* **15** 6017
[39] Siny I G, Tu C-S and Schmidt V H 1995 *Phys. Rev.* B **51** 5659
[40] Kamba S, Bovtun V, Petzelt J, Rychetsky I, Mizaras R, Brilingas A, Banys J, Grigas J and Kosec M 2000 *J. Phys.: Condens. Matter* **12** 497
[41] Buixaderas E, Kamba S and Petzelt J 2004 *Ferroelectrics* at press
[42] Petzelt J, Kozlov G V and Volkov A A 1987 *Ferroelectrics* **73** 101